Article:
Bailey, J, Clamp, J, Farmer, S et al. (5 more authors) (2022) Infrared triggered smart contact lens for the treatment of presbyopia. Journal of Physics D: Applied Physics. ISSN 0022-3727

https://doi.org/10.1088/1361-6463/ac52cc

Infrared triggered smart contact lens for the treatment of presbyopia

James Bailey[a), b)] *, John Clamp [c)], Steven Farmer[d)], Helen F Gleeson[b)], Tim Haynes[a)], J. Cliff Jones[b)], Tom Moorhouse[a)], and Philip Morgan[e)].

a) Dynamic Vision Systems, Nexus, Discovery Way, Leeds, LS2 3AA, UK.
b) School of Physics and Astronomy, University of Leeds, Woodhouse Lane, Leeds LS2 9JT, UK.
c) Ultravision CLPL, Leighton Road, Leighton Buzzard LU7 4RW, UK.
d) Pharmatechnics, E-space North Business Centre, 181 Wisbech Rd, Littleport, Ely, CB6 1RA, UK.
e) Eurolens Research, University of Manchester, Carys Bannister Building, Dover Street, Manchester M13 9PL, UK.

* Corresponding author: jbailey.physics@gmail.com

Keywords: Smart lens, switchable lens, contact lens, presbyopia, wearables, liquid crystal, electronics, switching speed

Tweetable abstract: Wire free switchable focus liquid crystal #SmartContactLens for the treatment of presbyopia.

Received : 30th September 2021
Accepted for publication: 8th February 2022

Abstract

A switchable contact lens prototype was fabricated and tested with integrated off the shelf electronic components to drive a liquid crystal active lens element. This prototype was capable of changing its focal power by an average of +1.9D, but a maximum of +3.2 ± 0.2D was also measured. Switchable focus contact lenses are intended to help restore functional near vision accommodation to those suffering from presbyopia, an inevitable age-related eye condition. The custom PMMA contact lens substrates used in this prototype are equivalent to commercially available scleral contact lenses. It was discovered that more careful design considerations are needed when at least one of the substrates is <100µm thickness (which is needed for a final device). Without these design considerations, the switchable focal power of the lens is susceptible to change as the liquid crystal insert layer is able to flex. The prototype has an on-board electronics platform which was self-powered with a battery. Illuminating the package with a 600Hz infrared signal switched the device on, which passed an AC voltage to the electrodes of the contact lens, reorientating the director of the liquid crystal with an electric field. To our knowledge, this is the first demonstration of a battery powered and wirelessly triggered smart contact lens for the treatment of presbyopia.

Introduction

Presbyopia is an inevitable eye condition that limits near vision accommodation and starts to progress at around forty years of age and affects nearly everyone over age fifty [1]. It is caused by an age-related reduction in crystalline lens flexibility, leading to a diminishing ability to focus on near objects clearly [1,2]. An estimated 1.8 billion people currently suffer from presbyopia and they will need some artificial vision correction to focus on near and

intermediate objects [3]. Presbyopia is the leading cause for people needing reading glasses and it has been shown to have a detrimental impact on people's quality of life [1]. A 2007 study had concluded that ten percent of those suffering with presbyopia considered the condition to be so detrimental that they would trade 5% of their remaining life for a cure [1]. Most sufferers require only 2.0D to 2.5D of additional optical correction to restore near vision ability [1]. Focal correction between 0 to 2.5D is also beneficial for visual accommodation at intermediate focal lengths. There is currently no cure for presbyopia that could restore vision to the same abilities as a young eye. The most effective treatments so far are corrective optics (spectacles or contact lenses) [1,2], multifocal lens replacement through eye surgery [4,5] and Supracor laser-assisted in-situ keratomileusis (LASIK) [5–7]. Multifocal spectacles are divided into regions dedicated to near, intermediate and far vision correction, typically with increasing positive lens focal power towards the lower parts of the lens. This enables the user to attain the necessary vision correction by directing their gaze through the appropriate region in the lens. A similar methodology is also applied to multifocal contact lenses, where regions are also dedicated to near, intermediate and far vision correction [8]. Contact lenses are positioned onto the surface of the eye, so it is not necessary for the wearer to switch focal power by altering their gaze. Instead, for most forms of multifocal contact lenses, the wearer experiences all the differing focal powered segments simultaneously. This may contribute to the greater drop-out rates that are seen with multifocal contact lenses when compared with other lens designs [9]. One recent report found a retention rate in the first year of multifocal soft contact lens use to be only 57%, which is significantly lower than toric (73%) or spherical (79%) contact lenses.

Smart contact lenses aim to overcome these issues by controllably changing their focal power with electronics. Nematic Liquid Crystals (LC) allow the refractive index of the lens material to be changed with only a few volts and minimal current. Several implementations have previously been proposed [10–24], and the work described here is based on the approach taken in previous research using a spherical LC lens shaped cavity [12–14,16,21–24]. Automatic triggering mechanisms (not yet tested) could enable these types of smart lenses to treat presbyopia seamlessly. This paper begins with discussing how the eye's crystalline lens focuses and how it could be compensated using a smart liquid crystal lens. Preparation of the liquid crystal lens, its performance and the associated on-board electronics platform used the drive the lens is detailed. Finally, routes for future improvements are then considered.

Eyes vary their focal power by changing the shape of the crystalline lens. This is equivalent to changing the radius of the lens, described by the lens-maker equation [25],

$$P = (n_2 - n_1)\left(\frac{1}{r_1} - \frac{1}{r_2}\right) \quad (1)$$

where P is the focal power, n_1 is the refractive index of the surrounding medium and n_2 of the lens, r_1 is the radius of the lens surface closest to the light source and r_2 is the second radius, as visualised in figure 1(a). Imitating a crystalline lens mechanism based on shape change, e.g. using flexible lens membranes [26–28] or electro-actuators [29–32], is difficult in equivalent man-made contact lens-sized devices. Instead, the birefringent and opto-electronic properties of liquid crystals are utilised by injecting it into a lens shaped cavity within the device [12–14,21–24]. Liquid crystals are formed from rigid rod-like molecules that orientate with a common direction, called the director, **n**. This leads to differing refractive indices along their ordinary (n_o) and extraordinary (n_e) axes, which are perpendicular and parallel to **n** respectively (illustrated in figure 1(b)). Reorienting the liquid crystal director, parallel to the direction of

incident light to perpendicular causes a decrease of the observed refractive index, as $n_o < n_e$ [33,34]. Figures 1(c) and 1(d) illustrate a negative meniscus liquid crystal lens layer, which is placed between two positive meniscus lenses with isotropic refractive indices. In this example, the total focal power is zero when the extraordinary refractive index of the liquid crystal layer n_e is experienced, illustrated in figure 1(c). Control of the liquid crystal configuration in the off state is achieved by a surface treatment that aligns the director parallel to the surface of the lens [33,34]. For a typical nematic liquid crystal with positive dielectric anisotropy, application of one to several volts to electrode layer on the lens causes the liquid crystal to reorientate parallel to the electric field direction, shown in figure 1(d) [33,34]. In a fully switched on state, only the n_o refractive index is experienced by the incident light, thereby reducing the magnitude of the negative focal power from the liquid crystal lens layer. Intermediate focal powers are possible by applying a controlled voltage so the refractive index is between n_o and n_e (discussed in the Method section). The total focusing power of the device is increased when the observed refractive index of the LC layer is reduced ($n_e \rightarrow n_o$), as the positive focal power of the non-liquid crystal lens layers is unchanged ($P_{Total} = P_{Lens1} + P_{LC} + P_{Lens2}$) [15].

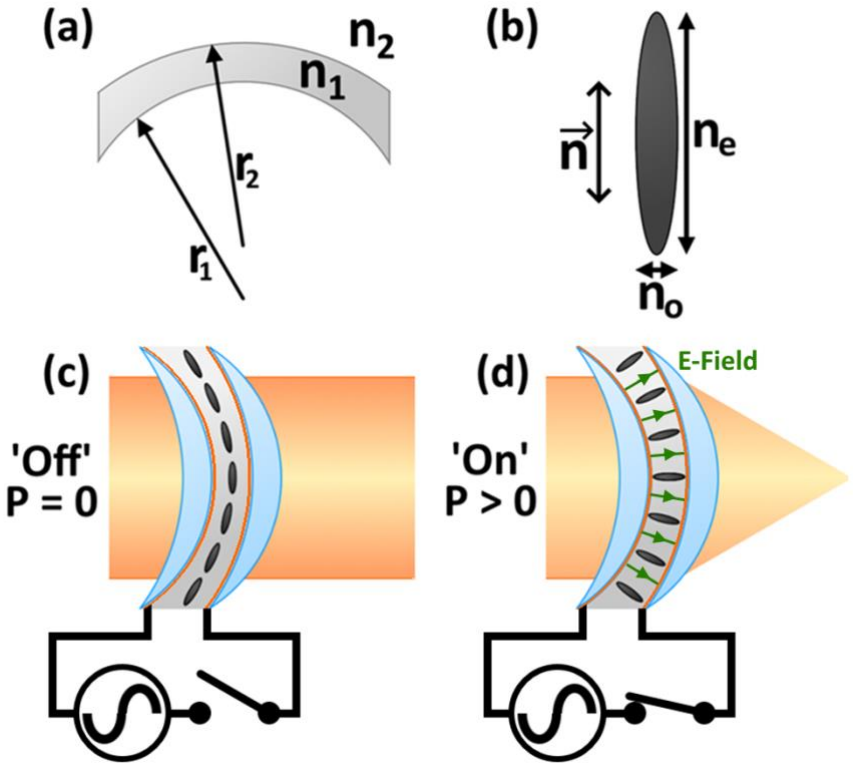

Figure 1: Illustration to demonstrate how a liquid crystal lens changes its focal power. (a) The liquid crystal is shaped into a lens. (b) Liquid crystals have differing refractive indices along their ordinary (n_o) and extraordinary (n_e) axes. (c) A lens system can be designed so it applies no additional focal power when the device is off. (d) An increase in focal power can be achieved by switching the device on, which lowers the magnitude of the negative focal power liquid crystal lens layer.

Different liquid crystal alignment modes and electrode materials have already been tested in previous research [12–14,16,21–24]. However, each of those lens devices were powered using external signal generators connected with wires to the lens. Here, we demonstrate a proof-of-concept device with integrated electronics that can be wirelessly triggered with an infrared signal. This prototype contains an internal battery to enable an entirely wire-free device. Other research groups have demonstrated battery [35] or supercapacitor [36] operated smart contact lenses for use in display applications. In addition,

the University of Ghent and Imec have developed a smart contact lens prototype that functions as an artificial iris to treat those with aniridia (eyes that have limited or no iris functionality) [37]. To our knowledge, our device is the first demonstration of a battery powered, wirelessly switching smart contact lens for the treatment of presbyopia.

Method

This prototype smart lens was adapted and improved from previously published designs [12–14,21–24] with the addition of an integrated electronics platform. As with that previous work, the lens substrates were made from poly-methyl-methacrylate (PMMA), which is a historical "hard" contact lens material with well understood properties. The substrates used here were designed to be equivalent to commercially available scleral contact lenses. Furthermore, the two substrates were split into two different sizes: a 'carrier-lens' and a 'capping-lens'. The carrier-lens, shown in figure 2(a), was large enough to accommodate both the smaller capping-lens and the electronics platform, within the diameter of a scleral contact lens (16mm). Both lens substrate sizes were fabricated using a high-precision Optoform-30 (Sterling Ultra Precision) contact lens lathe. The lens assembly without the electronics platform mounted onto its surface is shown in figure 2(b). A cross section illustration of the lens design is shown in figure 3, which includes the radii used in the optically active regions of the lens.

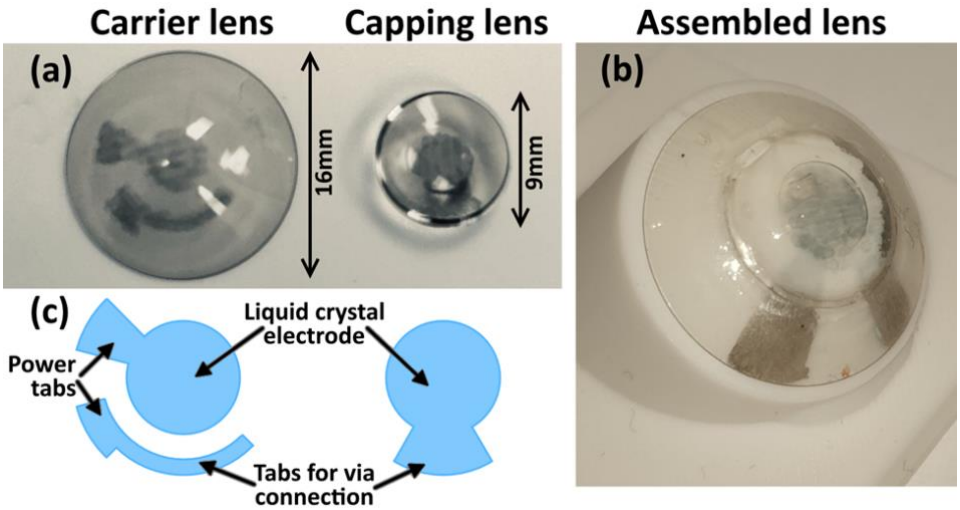

Figure 2: (a) PMMA contact lens substrates with polymer electrode layers printed onto their surface. Note that the contrast has been enhanced in this image to increase the visibility of the electrode. (b) Assembled contact lens without the electronics platform attached to its outer region. Contrast in this panel was not enhanced to increase the visibility of the electrode layers, but the two overlapping layers are visible from the carrier and capping-lens circular electrode regions. (c) Pattern of the polymer electrode layer, which was printed onto the contact lens substrate surfaces. This design enables the electronics platform to apply a voltage across the electrode layers by connecting to the power tabs.. The design uses a via connection to pass the voltage from the carrier-lens to the capping-lens, without short circuiting the device.

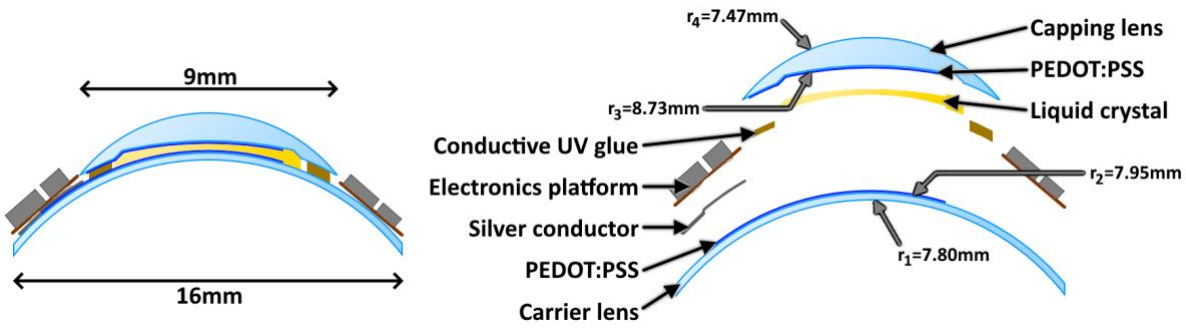

Figure 3: Illustrated schematic of the liquid crystal smart contact lens. The radii of the optical regions of the lens are also noted in this diagram. Both the carrier and liquid crystal lenses have a negative focal power and the capping lens has a positive focal power, but the total focal power was designed to be negligible when the device is off. The magnitude of the negative focal power liquid crystal layer decreases when the device is switched on, which increases the total focal power of the device.

The lens substrates were cleaned by sonicating them in Decon-90 soap/De-ionised (DI) water solution for 30 minutes followed by DI water for a further 30 minutes. Both substrates were dried with compressed air and, immediately before further processing, were placed into a UV ozone cleaner (T10X10/OES, UVOCS, USA) for 5 minutes to passivate their internal surfaces. The lenses were dip-coated by sonicating them again, but for 5 minutes in a 0.1% w.t. Poly(vinyl alcohol) (PVA, Sigma Aldrich, USA) in DI water solution. Both substrates were thoroughly dried using compressed air and placed onto a hotplate at 40°C for 20 minutes to ensure all residual water was evaporated. This process coated the lens substrates with a PVA layer, which helped them retain wettability and adhesion during the next process, inkjet printing. Poly(3,4-ethylenedioxythiophene) polystyrene sulfonate (PEDOT:PSS, Sigma Aldrich, USA) was used as the liquid crystal electrode layer and was deposited using a bespoke three-axis inkjet printer with a line width of 300 ± 50µm. Figure 2(c) shows the electrode layer patterns that were printed onto the lenses. The active area of overlap for the electrodes was 4mm in diameter, which is the same size the diameter of a pupil in a moderately lit room [38,39]. Connection tabs pass voltage to the carrier lens active electrode area and to the capping lens active electrode area using vias, which also helped prevent the device from short circuiting. An electronics platform connects to the power connection tabs, providing the voltage necessary for switching to the LC electrodes. Figure 4 illustrates the key components of the custom printer, which was built using linear stepper motor translation stages (Zapp Automation, UK), stepper motor driver (Zapp Automation, UK), 20µm diameter inkjet print head (MicroFab, USA), 3D printed parts, heat-mat (RS components, UK), Raspberry pi 3B+ board computer and HD camera (RS components, UK). A program written in Python was used to control the apparatus. This custom set-up enabled the inkjet head to follow the curved profile of the lens surface, which improved droplet deposition accuracy. Printing without following the lens profile (where the maximum space between print-head and lens substrate was 2mm) resulted in inkjet droplets depositing up to 1.5mm away from their intended position, which would cause the device to short-circuit. The PEDOT:PSS was diluted in DI water to 10% of its initial concentration, and an inline cellulose membrane filter with 5µm pore size was placed between the reservoir and inkjet head to prevent larger particulates jamming the nozzle. Two layers of PEDOT:PSS were printed to improve conductivity and uniformity, providing a sheet resistance of 380 ± 40 Ω/□) for the electrode layer. Optical transmittance had decreased by 6±1% after printing two layers of PEDOT:PSS onto the substrates. Transmittance of a fully assembled device had decreased by 12±2%, as PEDOT:PSS active electrode areas are needed on both the carrier and capping lens. Print quality was further improved by setting the heat-mat to 35±2°C during deposition, to promote water evaporation in the PEDOT:PSS thereby preventing

coalescence of the printed droplets. Both substrates were baked on a hotplate at 40ºC for half an hour to ensure the remaining water was evaporated from the PEDOT:PSS ink.

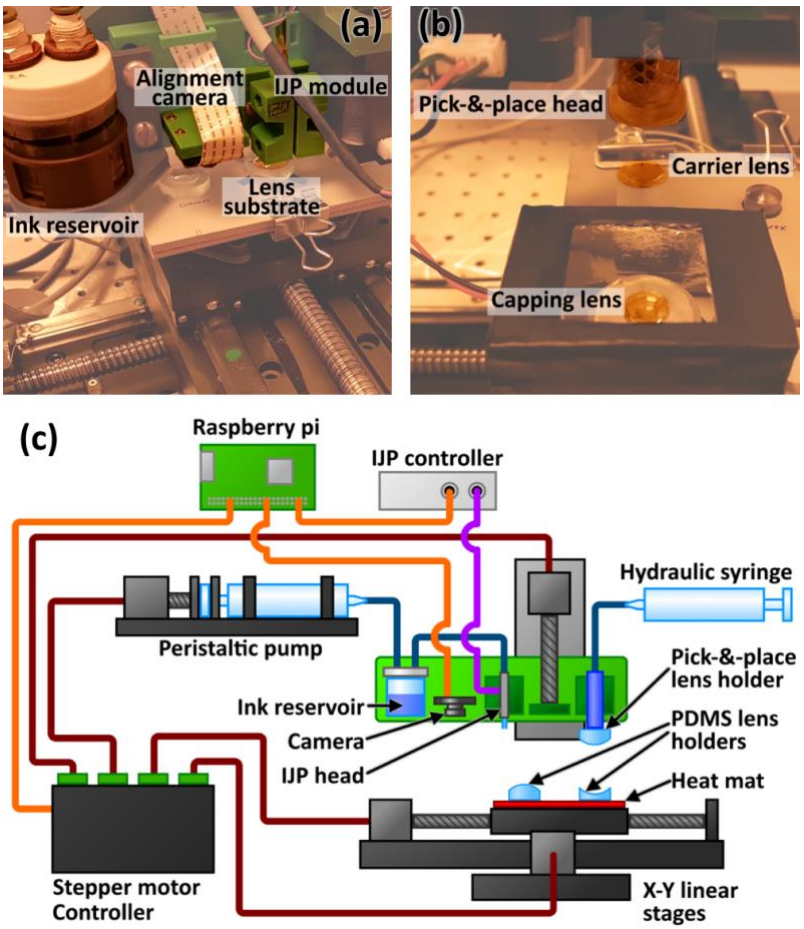

Figure 4: Custom made (a) inkjet printer and (b) lens assembly system, which removed most of the manual processing when building the prototypes. Schematic of the apparatus is illustrated in (c).

A PVA alignment layer was deposited on top of the PEDOT:PSS electrode layers using spin-coating as it did not require the time consuming and extensive patterning techniques of inkjet printing. This process used 1% wt. PVA (Sigma Aldrich, USA) dissolved into DI water, which was deposited onto the lens substrates while they were spinning at 3000 rpm for one minute. Depositing while spinning reduces the DI water contact time with the previously deposited PEDOT:PSS layers. Prolonged exposure to water would otherwise cause the PEDOT:PSS layer to crack and delaminate from the surface. These alignment layers were then dried on a 40ºC hotplate for half an hour to ensure all residual water was evaporated. Using a PVA alignment layer improved the longevity of the alignment when compared to using PEDOT:PSS as the alignment layer.

Anti-parallel alignment was applied to the lenses by rubbing their surfaces with a felt cloth, which creates uniform alignment of the pre-tilted director between the lens substrates. This alignment mode is consistent with previous LC lens experiments, which also used PEDOT:PSS as an electrode layer [13]. Additional alignment modes have been demonstrated previously, such as axial alignment [13]. However, planar alignment is significantly easier to apply and it is more widely adopted in liquid crystal devices.

UV glue (Norland 61, Thorlabs, USA) was doped with 2µm glass spacer beads and 5 µm gold conductive beads (0.1% wt. concentration) to provide 1D conductive via connection once the two lens substrates were laminated together under pressure. Automated pressurised

syringe deposition of the 1D conductive glue was attempted, but it was not possible to achieve sufficiently precise z-axis/height adjustment to ensure reliable processing for the internal surface of the lens. Instead, the doped glue was applied manually around the edges of the capping lens using a stylus.

The three-axis printer was designed as a modular system and a custom pick-and-place assembly arm was added to the set-up (illustrated in figure 4). This automated system increased the alignment and assembly reliability of the lens substrates, which reduced the risk of short-circuiting the device from a misaligned via connection. During assembly, sufficient pressure to indent the gold beads into the PEDOT:PSS electrodes and enable conduction to the connection tabs (illustrated in figure 2(c)) was applied. Once correctly assembled, the glue was cured by UV exposure for an hour. Long exposure times were needed to ensure that enough UV light had penetrated through the UV absorbing PMMA lens substrates. We were unable to use thermal curing glue for this lens application, as the PMMA lens substrates would deform when heated above 60ºC. Liquid crystal (E7, Synthon chemical, Germany) was forced into the lens cavity through the open hole in the glue seal using conventional vacuum filling [40]. The chemical composition of E7 is illustrated in figure 6). Non-conducting UV glue was then used to seal the small filling hole and prevent leakage of the liquid crystal. This was UV cured for 1 hour (again, due to PMMA substrate absorption), while also covering the liquid crystal cavity to limit its degradation. Uniform, monodomain liquid crystal alignment was observed when inspecting the devices with cross polarisation microscopy (Leica microscope, Germany) shown in figures 5(a) and 5(b). A purpose-built photodiode mounted onto the microscope, monochromatic light-source (λ=670nm), oscilloscope and signal generator were used to measure the response times of the liquid crystal.

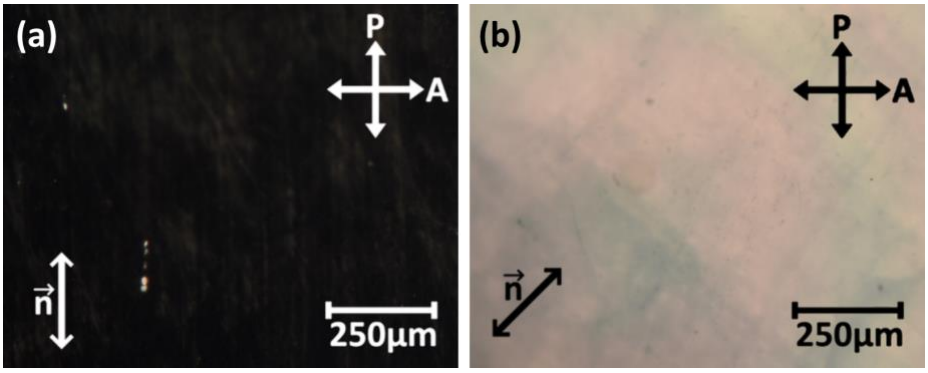

Figure 5: (a) Cross polarisation micrograph of liquid crystal contact lens. Director of the liquid crystal is parallel with the polariser (observing its dark state). (b) Cross polarisation micrograph of lens where director is orientated 45º to the polariser (observing its bright state).

The focal power of the contact lens changes when applying sufficient voltage to its electrode layers. We measured the change in focal power with respect to voltage using the optical set-up shown in figure 7(a). A 532 nm wavelength laser (Thorlabs, USA) was circularly polarised and expanded to the size of the 4mm radius active optic area of the liquid crystal contact lens. The laser light was then passed through a linear polariser, which could be rotated to match the alignment of the liquid crystal director in the contact lens. A linear polariser was necessary as the n_o refractive index is also observable when measuring the focal point from the n_e refractive index. The linear polariser is orientated parallel to the optic axis of the liquid crystal to remove the unwanted focal point caused by n_o when the lens is off. This polarised beam passes through the contact lens and then a plano-convex lens to focus the light onto the beam profile detector (Edmund Optics, UK). Polarisation dependence of single layer liquid crystal lenses is discussed in greater detail in reference [14]. An external signal generator was used to supply 1kHz sinusoidal test voltages between 0 and $7V_{rms}$. These wired tests are

comparable to previous liquid crystal contact lens experiments [12–14,22,23]. The proof-of-concept electronics package (discussed later) used off-the-shelf components, which can provide either 0V (when off) or a $4.1 \pm 0.2V_{rms}$ square wave (when on). This narrow bandwidth is why external electronics were used for these comprehensive voltage dependency tests. Specifically, for measuring the change in focal power with respect to changes in voltages and liquid crystal response times. An improved electronics package would enable multiple focal power modes, enabling dynamic accommodative response for intermediate vision correction (a proposed design is presented in the discussion section). The change in focal power with respect to applied voltage is shown in figure 7(b) for the liquid crystal material E7. At 20°C, this mixture has ordinary and extraordinary refractive indices of n_o = 1.524 and n_e = 1.748 respectively (Δn = 0.224) and a splay Fréedericksz threshold voltage of ~$0.77V_{rms}$. As eye temperature is around 34°C [41], a final lens design would benefit from a liquid crystal that is optimised to function at those higher temperatures, but E7 is an excellent first choice as its properties are relatively temperature-independent below ~50˚C.

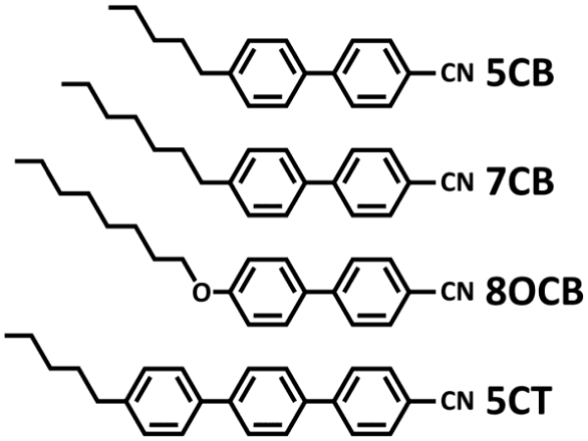

Figure 6: Illustration of the chemical composition used in the E7 liquid crystal mixture [42].

Results

Two separate prototypes were prepared and their focal powers were measured with respect to applied voltage. Both lenses were tested twice using the apparatus illustrated in figure 7(a). This largest and smallest changes in focal power were 3.2 ± 0.2D (Lens A) and 0.7 ± 0.2D (lens B) when these lenses reached their saturation voltages (shown in figure 7(b)). Despite these differences in focal power, both lenses were prepared using the same materials and techniques. Furthermore, different results were measured when re-testing the same lenses again under the same conditions (all within room temperature, 21 ± 2°C). These inconsistencies are explained by measuring the optical properties of the individual substrates. Table *I* lists the measured focal power of four different carrier and capping lenses of the same design. The capping lenses only vary their focal power by 0.6% between samples, whereas the carrier lens varied significantly by 11.3%. This is likely due to the amount of flex that the carrier lens may allow when compared to the capping lens. Specifically, the carrier lens was only 100µm thick at its centre, whereas the capping lens was 1000µm thick at its centre. The carrier lens was kept thin to retain its scleral lens likeness, which is important when considering future design iterations. This design choice has revealed fundamental challenges with LC lenses built on flexible substrates, which have not been presented elsewhere. The flexing of the lens components, particularly the carrier lens, occurred during the assembly process, as well as re-mounting of the lens during measurements. Possible methods to mitigate this problem in a final product is discussed later.

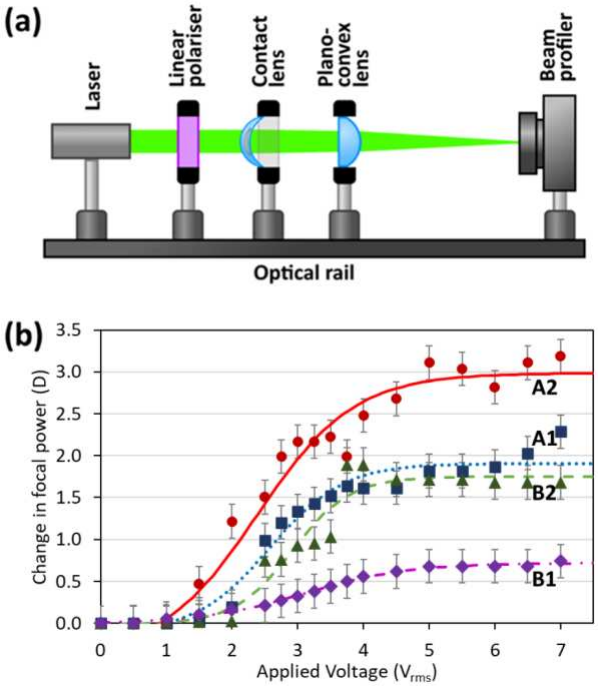

Figure 7: (a) Experimental setup for measuring the focal power of the liquid crystal contact lenses. (b) Change in focal power with respect to applied voltage to the contact lens electrodes. Two different lenses were tested twice, and a sigmoid function was used an approximated fit. These lenses are all the same design and they changed focal power when re-measured after mechanically flexing the lenses.

Table I: Focal power measurements of multiple lens substrates. The focal power of the capping lens is consistent between lens substrates. However, the focal power of the carrier-lens changed significantly between measurements.

Sample	Focal power (D)	
	Carrier lens	Capping lens
1	-1.076	10.753
2	-1.110	10.870
3	-1.183	10.753
4	-1.375	10.870
Average	-1.186	10.811
Standard deviation	0.134	0.067
Error (%)	11.29	0.62

The effect of variations in the carrier lens radii was modelled using equation (1) and the results shown in Figure 8. This shows that the carrier lens only needs to change its radius of curvature by less than ±600µm (which was ±8% of the lens radii) to account for the previously measured changes in focal power, as shown in figure 8(a). This degree of change is likely to occur from flexing of the thin plastic carrier lens substrate. Figure 8(b) shows the modelled changed in focal power and an assembled lens with respect to the carrier lens radius varying slightly. This modelled data also demonstrates that changes in carrier lens radius of less than ±7.5% are capable of causing the changes in switchable focal power previously measured (shown in figure 7(b)). Finally, the model shown in figure 8(c) was used to determine the degree of flexing of the bottom substrate that would be sufficient to electrically short circuit the device. The lowest cell spacing modelled (which is at the centre of the negative meniscus lens) was 6.5µm for measurement B2, so the devices were not at risk of short circuiting. Changes in the curvature of the carrier lens caused by flex and its impact on the focal power of

the device is illustrated in figure 9. These results highlight an important issue for *any* switchable contact lens: manufacturing reproducibility and sensitivity to optical differences induced through flexing the lens will occur without careful consideration.

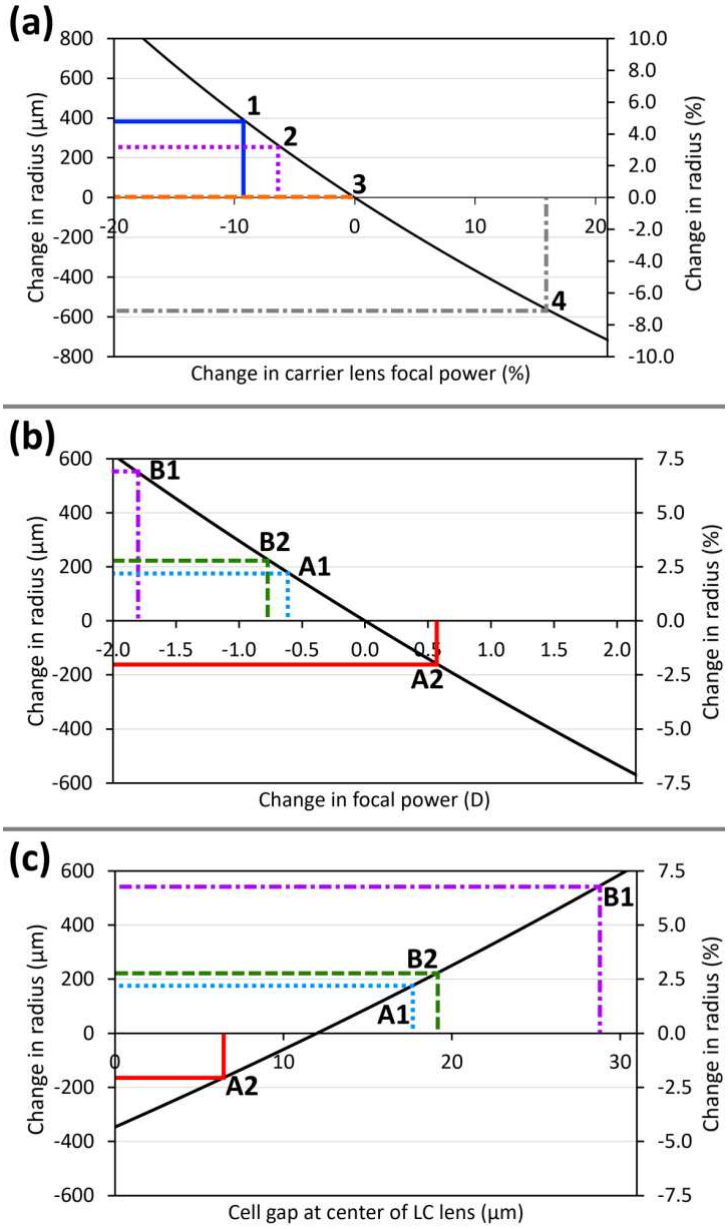

Figure 8: (a) Change in carrier lens focal power with respect to change in radii. Changes in lens radii of less than ±8% are enough to accommodate all the carrier lens focal power measurements, (b) Change in LC lens focal power with respect to changes in carrier lens radii. All 4 LC lens focal power measurements are within the tolerance of the carrier lens changes in radii, (c) Changes in LC lens cell gap with respect to change in lens radii. The model demonstrates that none of the measured LC lenses short circuit when the radius of the carrier lens changes.

Although untested in our prototype, two orthogonally aligned liquid crystal layers are the preferred approach for polarisation independence [14]. Figure 10 shows an illustration of how three substrates are needed to create two liquid crystal lens chambers. In this method, light transmitting through the lens will experience both n_e and n_o refractive indices, regardless of its polarisation orientation.

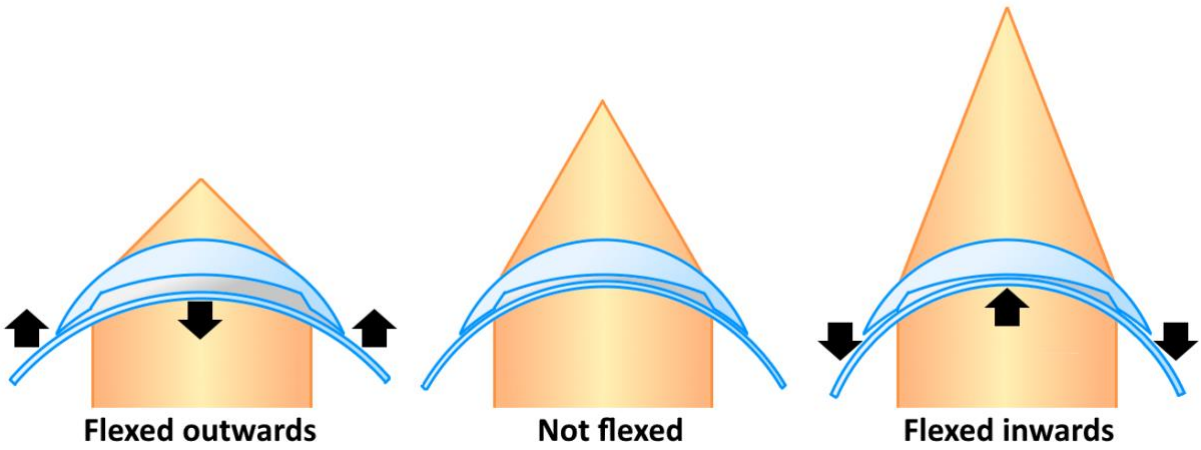

Figure 9: An exaggerated illustration of how the carrier lens flexing causes changes in the switchable focal power of the liquid crystal layer. Flexing the carrier substrate outwards (so it becomes flatter) reduces the magnitude of the negative meniscus liquid crystal layer, which increases total focal power. Likewise, flexing the carrier substrate inwards (so it comes rounder) increases the magnitude of the negative meniscus liquid crystal layer, which decreases total focal power.

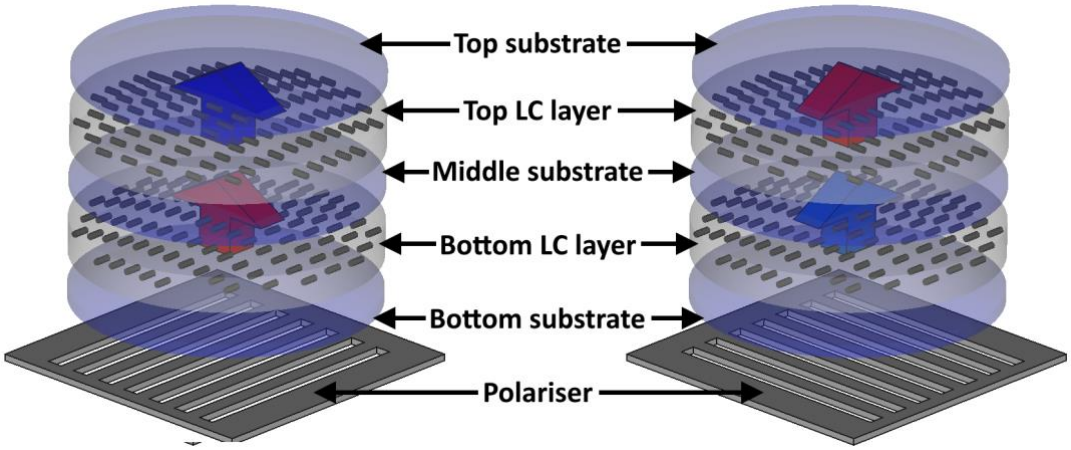

Figure 10: Illustration of achieving polarisation independence by aligning two liquid crystal lens layers orthogonal to one another. The blue/red arrows indicate when the polariser light is only experiencing the n_e/n_o refractive index respectively. Both the n_e and n_o refractive indices are equally experienced if the LC cavities are identical and the same liquid crystal is used.

Rigid contact lenses are typically less than 300µm thick for physical comfort and oxygen transport [43]. The lens material and oxygen transport method for future designs have not been decided, so 300µm is assumed in the following calculations. Each liquid crystal layer requires a cell gap of 35.5µm (for 2.5D from an LC with $\Delta n \approx 0.22$), which leaves 225µm for total lens substrate material. Therefore, the thickness of the substrate components used in a final design would be thinner than the 100µm thick carrier lens used in our proof-of-concept device. We have demonstrated that uncontrolled and greater changes in focal power will occur in a thinner and more flexible lens device. The contact lens will follow the shape of the eye, but this may not be sufficient to prevent changes in focal power from the cell gap sensitive LC layer. Possible solutions to overcome this challenge are provided in the discussion section.

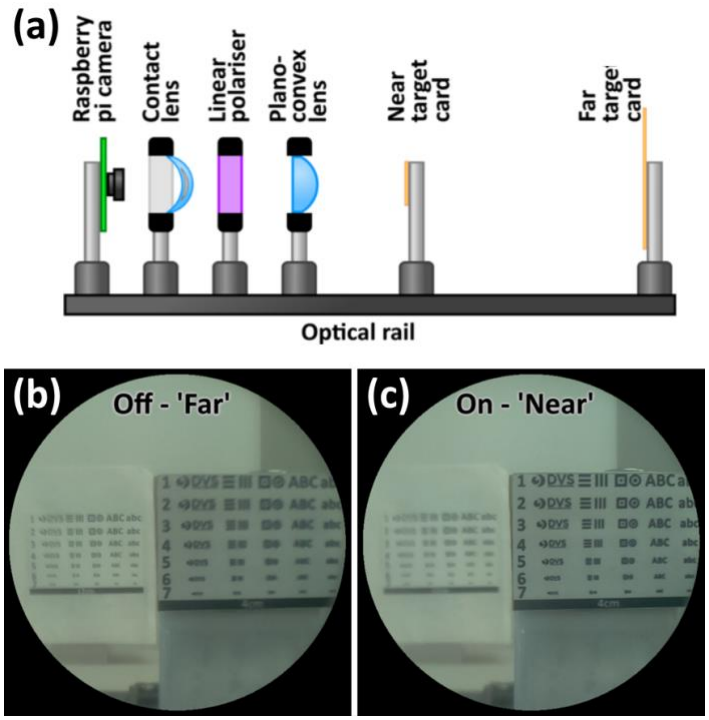

Figure 11: (a) Optical set-up when capturing images through the contact lens. (b) Image captured through the lens while it is unpowered and the 'far' targeted image is in focus. (c) Image captured through the lens when it is switched on and the 'near' targeted image is in focus.

The optics set-up, illustrated in figure 7(a), was re-arranged to include a Raspberry pi HD camera and two test card targets (illustrated in figure 11(a)). A 0.67D plano-convex lens was used in both images to compensate for the length of our experimental setup and bring the 'far' test card in focus when the device was off. These test cards used different images and letters to demonstrate the lens focusing. The 'far' and 'near' test cards were placed 150 ± 2cm and 40 ± 2cm away from the contact lens respectively. Note that the 'far' test card was 3x larger than the 'near' test card to keep it visible. Figure 11(b) shows that the text and patterns on the 'far' test card are in focus when the lens is off. Likewise, the text and patterns on the 'near' in focus when the lens is on. Both test cards were our own custom design. In near mode, the contact lens was able to distinguish the grouped lines in row 3 (line width, spacing and length were 0.35mm, 0.28mm and 1.58mm respectively). The lined features in row 4 were still distinguishable in the far image (line width, spacing and length were 1.05mm, 0.83mm and 4.73mm respectively). Contrast through this proof-of-concept device was reduced as 25±2% of light transmitting through the device is absorbed or scattered. Methods to improve transmission through future prototypes is discussed later.

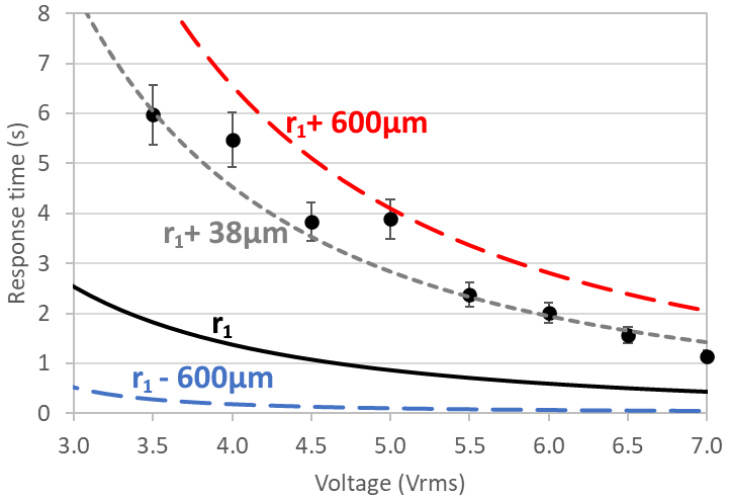

Figure 12: Measured response time of the liquid crystal when being switched into its on state. Switching time decreases when higher voltages are used. Expected response times for E7 were calculated for variations in the carrier lens radii (r_1 = 7.95mm) within the ±600µm tolerance of the carrier lens.

The response time of the liquid crystal lens was measured at different voltages, shown in figure 12. This prototype lens was able to switch within 1.1 ± 0.1s, when applying a $7V_{rms}$ driving voltage. The human eye takes 0.3s to initialise the visual accommodation and then an additional second to complete the process [44]. Therefore, the contact lens has a switching speed comparable to the human eye (which is approximately 1.3s). Lower voltages are necessary for switching the lens at smaller focal powers, but this will increase switching speed duration. Therefore, a 2-step switching process, where a large voltage is applied for a fraction of a second, may be necessary to maintain comparable switching speeds. The response time of the prototype was modelled using the following equation [45],

$$\tau_{on} = \frac{h_{max}^2 \, \eta}{\varepsilon_0 \, \Delta\varepsilon \, (V^2 - V_{th}^2)} \tag{2}$$

where h_{max} is the largest cell gap in the liquid crystal cavity, η is the relevant viscosity to the director reorientation of the liquid crystal, ε_0 is the vacuum permittivity, $\Delta\varepsilon$ is the dielectric anisotropy of the liquid crystal, V is the driving voltage applied to the liquid crystal and V_{th} is the threshold voltage of the liquid crystal. The following equation was used to calculate the largest cell gap in the lens [14], which was then inserted into equation 2,

$$h_{max} = h_0 + \Delta h = h_0 + r_1 - r_2 - \sqrt{r_1^2 - x^2} + \sqrt{r_2^2 - x^2} \tag{3}$$

where h_o is the smallest cell cap in the lens, (which is also the spacer height), Δh is the increase in cell gap due to the difference in curvature between the carrier and capping lens. The upper and lower ±600µm tolerances were added to figure 11 to demonstrate that the change in switching speed could be due to carrier substrate flexing. A modelled fit was achieved by applying a +38µm (+0.5%) offset to the carrier lens radii (r_1 = 7.95mm). Therefore, the switching speed is sensitive to cell gap, which can change when the substrate is flexed. Four different liquid crystals (MLC-6648, 5CB, E& and E44) were modelled to determine whether faster response times are achievable by changing material. Note that these liquid crystals have differing refractive indices, so the radii of the substrates would be different for optimised

lenses. The models were plotted with respect to maximum focal power to mitigate this problem when comparing data. All lenses showed that an increase in cell gap is necessary to achieve higher focal powers, which is linearly proportional. MLC-6648 has a lower birefringence ($\Delta n_{MLC\text{-}6648} = 0.07$) than the other liquid crystals, so it requires the carrier and capping lens to have a greater change in curvature, which increases cell gap (shown in figure 13(a)). There would be a small decrease in switching speed if we replaced E7 with 5CB or E44 in our prototype lenses (shown in figure 13(b)). However, the substrate curvatures would need to be re-optimised for those liquid crystals and the increase in speed is not significantly large.

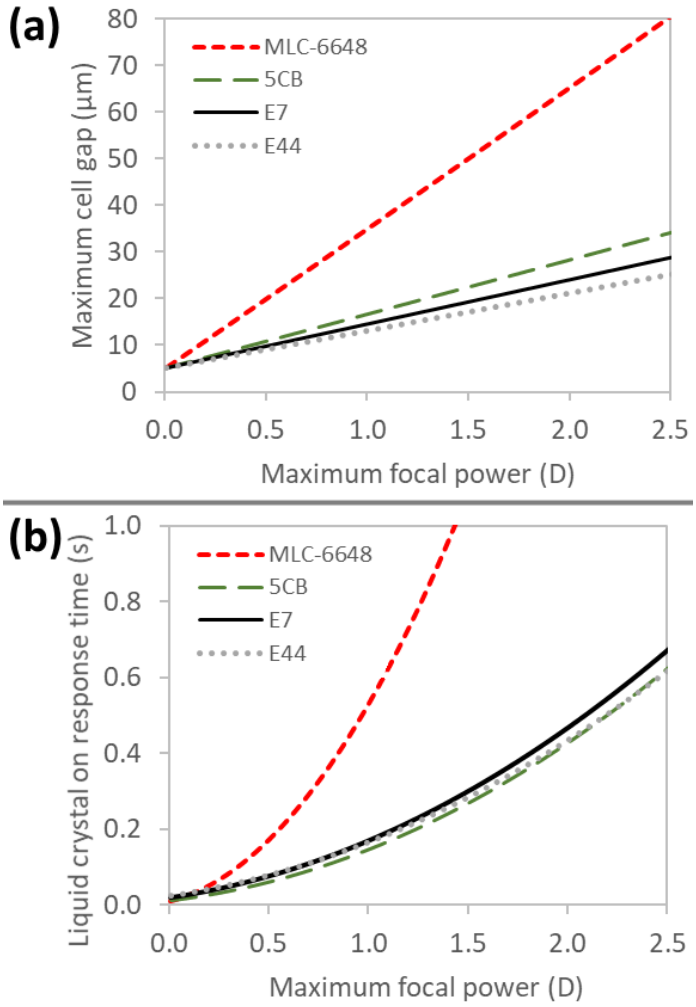

Figure 13: (a) Modelled data which illustrates the increase in cell gap necessary to achieve higher focal powers for 4 different liquid crystals. (b) Modelled data of on response time for 4 different liquid crystals with respect to maximum focal power.

The electronics platform was built as a proof-of-concept to demonstrate integrated on-board battery power and wireless switching in a smart contact lens. It was fabricated separately from the lens substrates, and then combined at the final assembly stages. This was developed using commercially available pre-packaged surface mount electronics to prove the current feasibility of operation using existing, low-cost components. However, restricting the design to off-the-shelf components results in the total thickness of the prototype being larger than a traditional contact lens. For example, the largest off-the-shelf components used in the prototype was a pre-packaged infrared receiver, with surface dimensions of 3mm x 2mm and a depth of 1mm [46]. The infrared receiver is too thick to fit into a 'standard' contact lens, but

it functions as intended in this proof-of-concept device. Further development of a commercial smart contact lens device will require small form factor/custom electronics to be procured to fit within the device, which will have significant design and tooling outlay. Custom electronics would also enhance the specialised functionality of these smart contact lens devices. An example of these types of electronics units suited for use in this application has already been developed by Imec and Ghent University [37,47], IMT Atlantique [48], as well as Mojo Vision [49].

A schematic of the electronics system prepared for the prototype and its operation is shown in figure 14(a). There are four main groups of components used to make the lens function:

- *Infrared receiver*: Wireless switching was built upon the use of an infrared receiver (Vishay semiconductors, USA). We chose infrared as a triggering mechanism, as it was simpler to integrate onto the lens electronics platform than other wireless methods that require an antenna, such as near field communication (NFC) induction and Bluetooth Low Energy (BLE). Infrared communication is readily achieved when restricted to using off-shelf packaged electronic components, which reduced the need for additional processing on-board the electronics platform. Furthermore, BLE requires 10mW when communicating with an external device [50], whereas the power used to communicate NFC and infrared receivers is required solely from the transmitting external device [50], thereby enhancing the battery life of the resultant lens. NFC induction antennas are only able to function a few centimetres away from the transmitter, whereas the infrared signal was able to transmit up to 30cm away from the smart-lens.

- *Band pass filter and amplifier*: The electrical signal from the infrared receiver was amplified and processed with a band pass filter. This preferentially selected the 1kHz infrared switching signal from the emitter and reduced the effects of infrared background noise (most notably 50/60Hz from low energy room lighting and 30-70kHz from domestic appliance remote controls). However, testing revealed that the lens was actually more efficient when it was being switched with a 600Hz infrared signal. An integrated oscillator on the electronics platform would use valuable space and increase the energy requirements of the device. Instead, the pulsed infrared signal from the transmitter was used to directly drive the oscillating signal in the circuit. Using this design results in the smart lens powering the LC electrode only while it was receiving a continuously pulsed infrared signal. Removing the pulsed infrared signal results in the lens switching off. A commercial device would not have this limitation, but this technique is suitable for this proof-of-concept prototype.

- *H-bridge driver*: Used to drive the 600Hz pulsed input bipolar antiphase signal so the output voltage has net zero DC balance and avoids unwanted ionic issues with the liquid crystal, as is customary for the driving of any LCD.

- *Solid state batteries*: The device was powered using two on-board re-chargeable solid-state batteries (5 µAh 3.8 V CBC005, Cymbet, USA) for wire-free operation [51]. Our modelling predicted that the electronics platform would drain 130 µA when switched on. Approximately 100 µA of this power is being consumed by a diode voltage pump used to drive the liquid crystal cell. These relatively large power requirements, needed

to drive the off-shelf components, result in an operational time of 2.3 minutes. This is smaller than that needed for daily operation, where recharging would be done overnight following > 10 hours of operation. In an optimised device, lower voltage liquid crystal materials would be used, thereby allowing the target +2.5 D change in optical power to be achieved without the need for the DC – DC converter. This would result in power consumptions significantly lower than 30μA and predicted battery lifetimes of over 10 minutes. Further improvements to significantly increase battery life are presented in the discussion section. Regardless, the current results still demonstrate this proof-of-principle devices as a battery powered switchable contact lens.

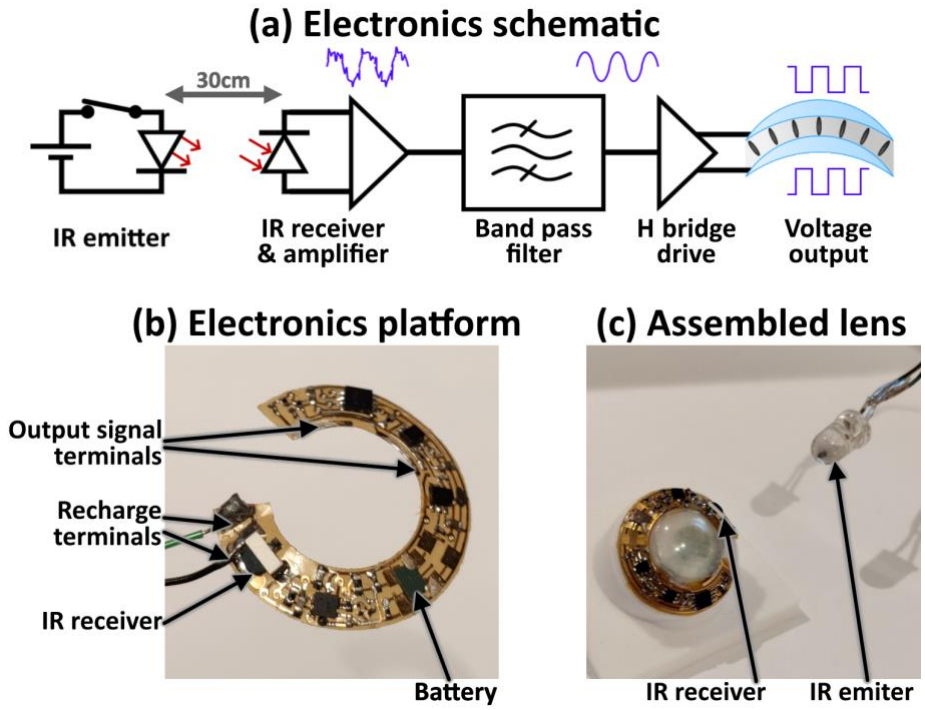

Figure 14: (a) Simplified schematic of the components used to drive the electronics platform, which passes its voltage output onto the electrodes of the contact lens substrate. (b) Copper etched Kapton film electronics platform populated with off-shelf components. (c) Assembled prototype with electronics platform mounted onto the carrier lens outer region and an IR emitter that was used for switching tests.

The lens receiver and driver units were prepared on an etched copper Kapton film substrate with off-the-shelf electronic components, shown in figure 14(b). The circuit was fabricated onto an annulus segment, which could be formed into a shallow truncated conical shape. Components were soldered onto the platform while it was pre-formed into the near-conical shape, reducing the risk of damage as the platform was subsequently fixed onto the lens carrier substrate. The output signal terminals of the electronics were attached to the power tabs of the contact lens substrate using silver doped conductive epoxy (Chemtronics, USA). This passes the output voltage of the electronics package, once triggered with the infra-red signal, onto the electrodes of the contact lens substrate which switches the liquid crystal. Non-conductive epoxy was used to secure the remaining regions of the electronics platform to the lens substrate. Wires were temporarily connected to the recharge terminals to charge the battery from a DC power-source. A final commercial device would not be re-charged using wire-terminals as all the electronics would be encased in a protective barrier. Instead, wireless methods would be used, such as charging through electric induction [52], photo-diode [53] or micro-electromechanical systems (MEMS) [54]. We speculate that one of these re-charge

systems could be integrated into an overnight lens cleaning system. Furthermore, photodiode and MEMS could be used to re-charge the lenses to extend their usability throughout the day.

A fully assembled lens is demonstrated in figure 15(a). The diameter and bottom surface of the prototype is the same as a scleral contact lens, but the device is currently too thick to comfortably put into the eye. Most of the packaged components on the electronics ring are ~1mm thick. Furthermore, the curved surface of the lens and the profile of the electronics package do not perfectly meet throughout. This causes the electronics package to protrude slightly (by ~0.5mm) over the outer regions of the lens. The electronics segments of the lens prototype were coated in UV glue (Norland 61, Edmund optics, UK) and then manually re-cut with a lathe, shown in figure 15(b). This resulted in the prototypes having a thickness of 2.2 ± 0.3mm (shown in figure 15(c), which is larger than the 0.3mm maximum thickness of comfortable contact lenses [39,43]. This prototype still functions as a proof-of-principle device, as it is approximately the same form-factor as a traditional contact lens.

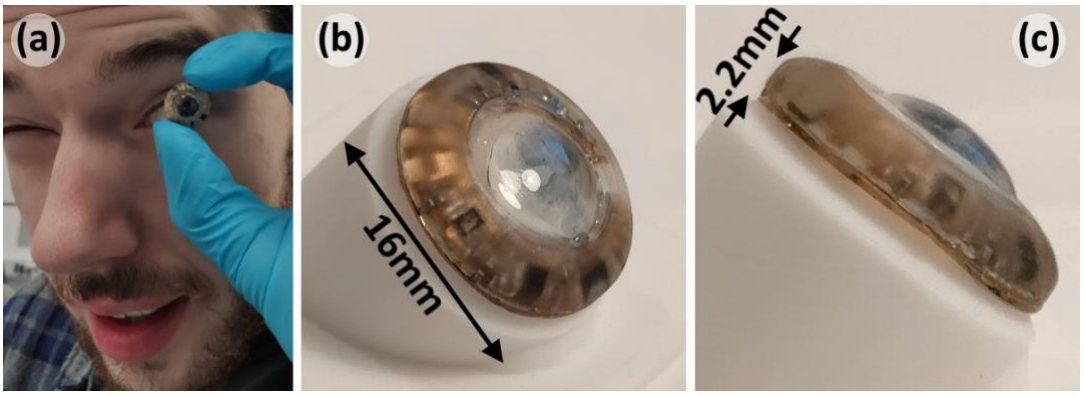

Figure 15: (a) One of the contact lens prototypes being demonstrated. (b) The contact lens prototype after it has been coated in UV glue and re-cut using a lathe. (c) Side profile of the re-cut contact lens, showing that it is too thick to comfortably put into an eye, but it is still compact.

Discussion

Using a carrier lens that was of a similar thickness to a standard scleral contact lens has revealed new challenges when trying to maintain consistent switchable optical properties. This is due to the thin lens substrate being able to flex, which distorts the shaped liquid crystal lens insert layer. Therefore, methods to retain the shape of the liquid crystal lens insert layer should be considered for future prototypes, which are discussed below (also illustrated in figure 16):

(a) *Adhesive pillars*: The shape of the lens substrates is braced together using adhesive pillars. A single central pillar may be enough to restrain the lens deformation, or an array of pillars may be needed. Visual imperfections created by these pillars could be reduced by index matching them close to the liquid crystal and keeping pillar density low. Although, the presence of the pillars may disturb the alignment of the liquid crystal, but further investigation is required. Photo-spacers on flexible lens substrates has already been demonstrated by J De Smet et. Al., but those devices where not designed as focusing devices [55,56].

(b) *Polymer stabilisation*: The liquid crystal is loaded with a polymer stabiliser, which is then cured with UV light while the lens is braced in a transparent mould. This will increase the voltages needed to drive the liquid crystal in the lens, but it could be necessary to maintain consistent optical performance. Polymer stabilisation has already been demonstrated for Fresnel lens

designs [17,57–59], but it has not been demonstrated as a method to brace together flexible substrates into a spherical contact lens shape.

(c) *Lens annulus*: A 1mm diameter anterior polar cataract, which is an opaque defect in the middle of the eye-cataract, doesn't reduce vision quality [60]. The central 1mm region of the contact lens could be re-purposed for bracing the device together. Therefore, the liquid crystal lens layer is shaped into a lensing annulus instead of a spherical lens shape. The central region of the contact lens could be dedicated to a contact lens display (demonstrated by Mojo Vision's prototype [49]) and / or a proximity sensor to assist with automated lens switching.

(d) *Rigid lens insert*: Only the lensing regions of the device need to be rigid to maintain optical quality. The other regions of the lens can be flexible, which would also increase comfort. Therefore, the central lens component could be made from a material that is tougher than PMMA, while the outer regions of the device are made from a flexible material (such as a hydrogel).

(e) *Regulating voltage*: It may not be possible to prevent the liquid crystal lens from changing its focal power due to small changes in cell gap from flexing. Instead, the lens may need to control its focal power by regulating the voltage being applied to the liquid crystal layer. This would require additional sensors and a feedback loop system to maintain the desired optical power.

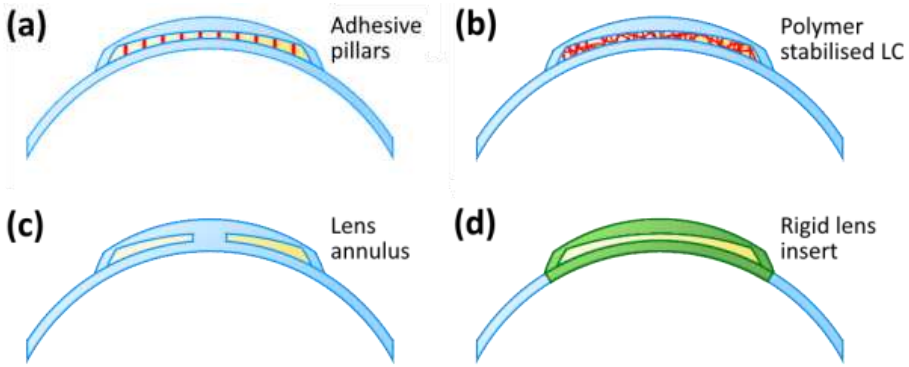

Figure 16: Suggested methods to maintain the curvature of the liquid crystal contact lens (a) Adhesive spacer pillars are used to brace the lens together. (b) Lens is polymer stabilised to retain its shape. (c) Central region of the lens is dedicated to improving the rigidity of the device. The lens is formed into an annulus instead of a spherical lens shape. (d) The centre of the device is made from a very rigid material and the outer 'skirt' is made from a flexible material to retain comfort.

A large number of improvements are also recommended to move the proof-of-concept device towards a commercial device, as discussed below.

- *Low voltage liquid crystal mixture*: There are more power efficient liquid crystal materials that can operate at lower voltages than E7. For example, MLC-6204 would have a better electrical power efficiency than E7, due to its high dielectric anisotropy and low elastic constants, but it has a lower birefringence and therefore requires a higher lens curvature for the same optical power. Therefore, investigations into a bespoke liquid crystal that balances power efficiency and optical performance are desirable.

- *Low power electronics*: The short battery life of the prototype was lower than the >10 hours operation that may be needed for a day's use. It is not feasibly possible to significantly

increase the size of the battery on the smart contact lens due to safety. Instead, far more energy efficient custom electronics should be designed specifically for the smart contact lens. This would be similar to the custom electronics demonstrated by Imec [37,47] and Mojo Vision [49]. However, the solution explored for the present work was to use all-polymer electronics from Pragmatic IC due to its reduced cost (when compared with developing and preparing equivalent silicon ASICs) and flexibility. Using their process design kit, it was calculated that the electronics could be prepared on a 4mm^2 low power custom ASIC chip. This would represent a major reduction in lens thickness, and to wearable prototypes suitable for product testing and medical trials.

- *Low energy communication*: Low energy Bluetooth and WiFi require too much power for practical use in smart contact lens devices [50]. Instead, a bespoke low power wireless communication system is being developed, using a Planar inverted F-antenna as shown in figure 17(a). A 5GHz radio frequency was used to minimise antenna size, while also maximising power efficiency. This type of antenna is able to function while placed on top of materials with a high dielectric contact (such as a human eye), which would de-tune most other antenna types [61].

- *Energy recovery*: The electrode layers in a liquid crystal cell function similar to charging capacitors. However, unlike the dielectric used in capacitors the polarity of the electrodes in the LC need to continuously switch to prevent ionic breakdown of the LC. This continuous switching is energy inefficient without careful design. A method of storing and re-using the discharged energy in the lens is in development, which stores recovered energy at discrete voltage steps, as illustrated in figure 17(b). This will enable the device to have pre-programmed focal power switching intervals of +0.25D.

- *Polarisation independence*: Modifying the design of the device with orthogonally aligned dual LC layers [14], or more sophisticated polarisation independent arrangements such as J.C. Jones et. al. [16].

- *Improved optical transmission*: PEDOT:PSS was chosen as the electrode material for this prototype because of the simplicity of creating the required electrode patterns using additive manufacturing. However, the PEDOT:PSS used absorbed 6±1% of light passing through each electrode layer. A polarisation independent device using two liquid crystal layers would require four electrode layers. Using the same PEDOT:PSS inkjet printed system as the initial prototype would result in a loss in transmission of approximately 22%, which would be detrimental to the optical performance of the contact lens. Therefore, metal nano-wires should be added to the PEDOT:PSS electrode layer using inkjet printing or photolithography [62,63]. Adding metal nanowires will increase the conductivity of the electrode material, which will require less material to be deposited while retaining the same switching performance. Adding metal nanowires to PEDOT:PSS has demonstrated sheet resistances of 55Ω/□, with optical losses of 7% [62]. The undoped PEDOT:PSS layers used in our prototype had a sheet resistance 7x greater than the metal nano-wire doped PEDOT:PSS films reported by Mayousse, et al [62]. Therefore, we estimate that the transmission loss from the each electrode layer could be as low as 1% by modifying the PEDOT:PSS layer with metal nano-wires [62,63]. A dual layer polarisation independent liquid crystal lens could lose only 4% of light transmitting through the device because of its electrode layers.

- *Oxygen permeability*: Our lenses were prepared on PMMA, as its properties are well known and it has historically been used as a contact lens material. However, its hydrophobic properties prevent oxygen from permeating through the material, which results in the eye asphyxiating during contact lens use. This results in corneal swelling, making the prototype impractical to wear without improvements. Imec [37] and Mojo Vision [60] have already demonstrated smart contact lenses that enable oxygen permeability by using rigid gas permeable materials for their lens substrates.

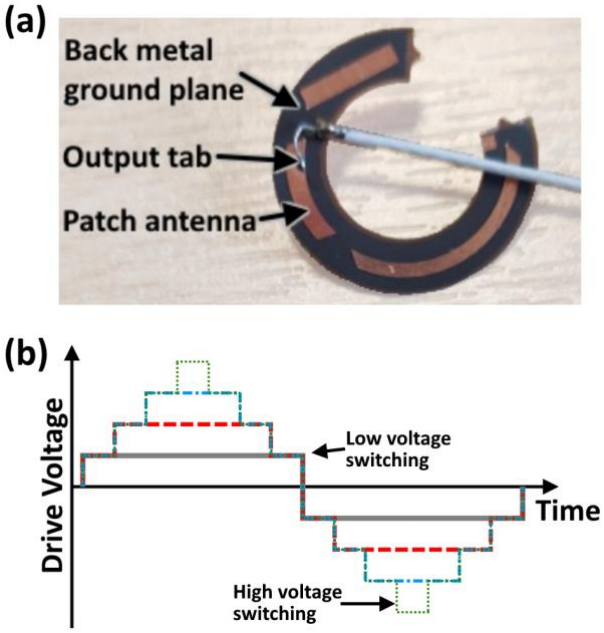

Figure 17: (a) Planar inverted F antenna prototype, which was able to function at 5GHz while placed on a pig's eye (as an approximation to a human eye). (b) Schematic of the voltage profile used in the discharge energy recovery system to reduce energy used when driving the liquid crystal cell within the smart contact lenses.

Conclusion

A contact lens proof-of concept device is reported to demonstrate wireless switching and on-board battery powered operation using off the shelf components. The lens can exceed the 2D focussing correction required for the great majority of presbyopia sufferers [1]. For example, 2D would provide a 50cm focal length (close enough to read a newspaper). This prototype is closer to a final product than any other reported so far. Reducing the thickness of the substrates further and shaping them into a scleral contact lens had highlighted a number of limitations that need to be addressed in future development. Specifically, the discovery that thin substrates can flex, which changes the switchable focal power of a liquid crystal lens insert layer. Possible improvements have been discussed which includes improved LC lens designs and electronics. As such, this prototype has revealed these additional challenges, whilst still being an important and significant step beyond previous switchable contact lens devices [12–14,21–24], which had no integrated electronics in their design. Response time measurements concluded that the lens has a switching speed equivalent to the human eye. Additional modelling was calculated to demonstrate how sub substrate flexing will also change the switching speed of the device. Switching speed for alternative liquid crystals was also calculated, but it was concluded that significant gains are not achievable with liquid crystals that are not highly specialised. The device had an average change in focal power of +1.9D, but this also varied has high as an additional 1.3D (+68%) due to substrate flexing. Contact lenses

are available in incremental focal powers of ±0.25D. Therefore, the liquid crystal lenses need to be optically consistent within ±6% to be comparable to traditional contact lenses. The methods disclosed in the discussion section are intended to overcome the challenges encountered when using thin substrates that flex to try and achieve better optical consistency. Regardless, this device acts as a successful proof-of-principle that demonstrates it is possible for smart contact lenses to discretely restore near vision accommodation to those that suffer from presbyopia and improve their quality of life.

Acknowledgements

The authors would like to thank The Universities of Manchester and Leeds, Innovate UK, IP Group and Parkwalk Investment for their investment into Dynamic Vision Systems. Thanks, is also given to the University of Leeds for use of laboratory spaces and facilities. We would also like to thank Stuart Weston and his mechanical workshop team at the University of Leeds for preparing sample components, which were later cut using the contact lens lathes at Ultravision. JCJ wishes to acknowledge the support from EPSRC through an Advanced Fellowship in Manufacturing (EP/ L015188/2 and EP/S029214/1).

Data availability

The data that support the findings of this study are available from the corresponding author upon reasonable request.

References

[1] Luo B P, Brown G C, Luo S C and Brown M M 2008 The Quality of Life Associated with Presbyopia *Am. J. Ophthalmol.* **145** 618–22

[2] Morgan P B and Efron N 2009 Contact lens correction of presbyopia *Contact Lens Anterior Eye* **32** 191–2

[3] Fricke T R, Tahhan N, Resnikoff S, Papas E, Burnett A, Ho S M, Naduvilath T and Naidoo K S 2018 Global Prevalence of Presbyopia and Vision Impairment from Uncorrected Presbyopia: Systematic Review, Meta-analysis, and Modelling *Ophthalmology* **125** 1492–9

[4] Greenstein S and Pineda II R 2016 The Quest for Spectacle Independence: A Comparison of Multifocal Intraocular Lens Implants and Pseudophakic Monovision for Patients with Presbyopia *Semin. Ophthalmol.* **32** 111–5

[5] Wolffsohn J S and Davies L N 2019 Presbyopia: Effectiveness of correction strategies *Prog. Retin. Eye Res.* **68** 124–43

[6] Mehrjerdi M A Z, Mohebbi M and Zandian M 2017 Review of static approaches to surgical correction of presbyopia *J. Ophthalmic Vis. Res.* **12** 413–8

[7] Ang R E, Reyes R M M and Solis M L P 2015 Reversal of a presbyopic LASIK treatment *Clin. Ophthalmol.* **9** 115–9

[8] Madrid-Costa D, García-Lázaro S, Albarrán-Diego C, Ferrer-Blasco T and Montés-Micó R 2013 Visual performance of two simultaneous vision multifocal contact lenses *Ophthalmic Physiol. Opt.* **33** 51–6

[9] Sulley A, Young G and Hunt C 2017 Factors in the success of new contact lens wearers *Contact Lens Anterior Eye* **40** 15–24

[10] Blum R D, Haddock J N, Kokonaski W and Hunkeler J 2008 Flexible Dynamic Electro-Active Lens (Patent No. US 9155614 B2) 1–22

[11] Sato S, Sugiyama A and Sato R 1985 Variable-focus liquid-crystal fresnel lens *Jpn. J.*

Appl. Phys. **24** L626–8
[12] Kaur S, Kim Y-J, Milton H, Mistry D, Syed I M, Bailey J, Novoselov K S, Jones J C, Morgan P B, Clamp J and Gleeson H F 2016 Graphene electrodes for adaptive liquid crystal contact lenses *Opt. Express* **24** 8782–7
[13] Bailey J, Kaur S, Morgan P B, Gleeson H F, Clamp J H and Jones J C 2017 Design Considerations for Liquid Crystal Contact lenses *J. Phys. D Appl. Phys. JPhysD* **50**
[14] Bailey J, Morgan P B, Gleeson H F and Jones J C 2018 Switchable Liquid Crystal Contact Lenses for the Correction of Presbyopia *Crystals* **8** 24
[15] Milton H E and Van Heugten A 2019 Developments in Electroactive Lens Technology for Vision Correction *SID Symp. Dig. Tech. Pap.* **50** 989–91
[16] Jones J C, Wahle M, Bailey J, Moorhouse T, Snow B and Sargent J 2019 Polarisation independent liquid crystal lenses using embossed reactive Mesogens *Dig. Tech. Pap. - SID Int. Symp.* **50** 992–5
[17] Fan Y-H, Ren H and Wu S-T 2003 Switchable Fresnel lens using polymer-stabilized liquid crystals *Opt. Express* **11** 3080
[18] Li G, Mathine D L, Valley P, Ayräs P, Haddock J N, Giridhar M S, Williby G, Schwiegerling J, Meredith G R, Kippelen B, Honkanen S and Peyghambarian N 2006 Switchable electro-optic diffractive lens with high efficiency for ophthalmic applications. *Proc. Natl. Acad. Sci. U. S. A.* **103** 6100–4
[19] Valley P, Mathine D L, Dodge M R, Schwiegerling J, Peyman G and Peyghambarian N 2010 Tunable-focus flat liquid-crystal diffractive lens *Opt. Lett.* **35** 336
[20] Li L, Bryant D and Bos P J 2014 Liquid crystal lens with concentric electrodes and inter-electrode resistors *Liq. Cryst. Rev.* **2** 130–54
[21] Milton H E, Gleeson H F, Morgan P B, Goodby J W, Cowling S and Clamp J H 2014 Switchable liquid crystal contact lenses: dynamic vision for the ageing eye *Proc. of SPIE* vol 9004, ed L-C Chien, A M Figueiredo Neto, K Neyts and M Ozaki p 90040H
[22] Milton H E, Morgan P B, Clamp J H and Gleeson H F 2014 Electronic liquid crystal contact lenses for the correction of presbyopia *Opt. Express* **22** 8035
[23] Syed I M, Kaur S, Milton H E, Mistry D, Bailey J, Morgan P B, Jones J C and Gleeson H F 2015 Novel Switching Mode in a Vertically Aligned Liquid Crystal Contact Lens *Opt. Express* **23** 9911–6
[24] Milton H E, Kaur S, Jones J C, Gleeson H F, Morgan P B and Clamp J 2014 Liquid Crystal Device and Method of Manufacture (Patent No. US 10459128 B2) 1–44
[25] Hecht E 2008 *Optics* (Boston, United States: Addison Wesley)
[26] Sugiura N and Morita S 1993 Variable-focus liquid-filled optical lens *Appl. Opt.* **32** 4181–6
[27] Zhang D-Y, Justis N, Lien V, Berdichevsky Y and Lo Y-H 2004 High-performance fluidic adaptive lenses *Appl. Opt.* **43** 783
[28] Ren H, Fox D, Anderson P A, Wu B and Wu S-T 2006 Tunable-focus liquid lens controlled using a servo motor *Opt. Express* **14** 8031
[29] Schneider F, Draheim J, Kamberger R, Waibel P and Wallrabe U 2009 Optical characterization of adaptive fluidic silicone-membrane lenses *Opt. Express* **17** 11813
[30] Wei K, Domicone N W and Zhao Y 2014 Electroactive liquid lens driven by an annular membrane *Opt. Lett.* **39** 1318
[31] Li J, Wang Y, Liu L, Xu S, Liu Y, Leng J and Cai S 2019 A Biomimetic Soft Lens Controlled by Electrooculographic Signal *Adv. Funct. Mater.* **29** 1–8
[32] Ghilardi M, Boys H, Török P, Busfield J J C and Carpi F 2019 Smart Lenses with Electrically Tuneable Astigmatism *Sci. Rep.* **9** 1–10
[33] Kumar S 2000 *Liquid Crystals* (Cambridge, UK: Cambridge University Press)
[34] Goodby J W, Collings P J, Kato T, Tschierske C, Gleeson H F and Raynes P 2014

Handbook of Liquid Crystals (Weinheim, Germany: Wiley-VCH)
[35] Nasreldin M, Delattre R, Ramuz M, Lahuec C, Djenizian T and De Bougrenet De la Tocnaye J L 2019 Flexible micro-battery for powering smart contact lens *Sensors (Switzerland)* **19** 1–7
[36] Park J, Ahn D B, Kim J, Cha E, Bae B S, Lee S Y and Park J U 2019 Printing of wirelessly rechargeable solid-state supercapacitors for soft, smart contact lenses with continuous operations *Sci. Adv.* **5** 1–9
[37] Vásquez Quintero A, Pérez-Merino P and De Smet H 2020 Artificial iris performance for smart contact lens vision correction applications *Sci. Rep.* **10** 1–12
[38] Winn B, Whitaker D, Elliott D B and Phillip N J 1994 Factors Affecting Light-Adapted Pupil Sizein Normal Human Subjects *Investig. Ophthalmol. Vis. Sci* **35** 1132–7
[39] Charman W N 2017 Correcting presbyopia: the problem of pupil size *Ophthalmic Physiol. Opt.* **37** 1–6
[40] Shimotoyodome G and Sugiura I 1996 Process for filling liquid crystal by gradually easing the level of negative pressure (Patent No. US 5751392) 1–6
[41] Morgan P B, Soh M P, Efron N and Tullo A B 1993 Potential Applications of Ocular Thermography *Optom. Vis. Sci.* **70** 568–76
[42] Anon 2021 Product Specification sheet: Liquid crystal mixture E7
[43] Gardner H P, Fink B A, Mitchell L G and Hill R M 2005 The Effects of High-Dk Rigid Contact Lens Center Thickness, Material Permeability, and Blinking on the Oxygen Uptake of the Human Cornea *Optom. Vis. Sci.* **82** 459–66
[44] Charman W N 2008 The eye in focus: Accommodation and presbyopia *Clin. Exp. Optom.* **91** 207–25
[45] Jones J C 2017 *Liquid crystal displays in Handbook of Optoelectronics* ed D J P and R G W Brown (CRC Press)
[46] Vishay Semiconductors 2021 Specification sheet - VEMD10940FX01
[47] Vásquez Quintero A, Verplancke R, De Smet H and Vanfleteren J 2017 Stretchable Electronic Platform for Soft and Smart Contact Lens Applications *Adv. Mater. Technol.* **2**
[48] Khaldi A, Daniel E, Massin L, Kärnfelt C, Ferranti F, Lahuec C, Seguin F, Nourrit V and de Bougrenet de la Tocnaye J L 2020 A laser emitting contact lens for eye tracking *Sci. Rep.* **10** 1–8
[49] Kastrenakes J and Carman A 2020 This startup wants to put a tiny display on a contact lens *The Verge*
[50] Mannion P 2017 Comparing Low-Power Wireless Technologies (Part 1) *Digi-Key Electron.*
[51] Anon 2016 EnerChip™ Bare Die - Specification sheet *Cymbet Corp.* 1–13
[52] Lingley A R, Ali M, Liao Y, Mirjalili R, Klonner M, Sopanen M, Suihkonen S, Shen T, Otis B P, Lipsanen H and Parviz B A 2011 A single-pixel wireless contact lens display *J. Micromechanics Microengineering* **21**
[53] Pletcher N and Otis B 2012 Contact lenses with Hybrid Power Sources (Patent No. US 2014/0192311 A1) 1–16
[54] Pugh R B, Riall J D, Toner A and Flitsch F A 2014 Variable optic ophthalmic device including liquid crystal elements (Patent No. US 2015/0138454A1) 1–40
[55] De Smet J, Avci A, Joshi P, Cuypers D and De Smet H 2012 A Liquid Crystal Based Contact Lens Display Using PEDOT : PSS and Obliquely Evaporated SiO2 *SID 2012* pp 1375–8
[56] De Smet J, Avci A, Joshi P, Schaubroeck D, Cuypers D and De Smet H 2014 Progress toward a liquid crystal contact lens display *J. Soc. Inf. Disp.* **21** 399–406

[57] Lin Y H, Wang Y J and Reshetnyak V 2017 Liquid crystal lenses with tunable focal length *Liq. Cryst. Rev.* **5** 111–43
[58] Hsu C J and Sheu C R 2012 Using photopolymerization to achieve tunable liquid crystal lenses with coaxial bifocals *Opt. Express* **20** 4738
[59] Ren H, Fan Y H, Gauza S and Wu S T 2004 Tunable microlens arrays using polymer network liquid crystal *Opt. Commun.* **230** 267–71
[60] Ionides A, Berry V, MacKay D, Shiels A, Bhattacharya S and Moore A 1998 Anterior polar cataract: Clinical spectrum and genetic linkage in a single family *Eye* **12** 224–6
[61] El Gharbi M, Fernández-García R, Ahyoud S and Gil I 2020 A review of flexiblewearable antenna sensors: Design, fabrication methods, and applications *Materials (Basel).* **13** 1–18
[62] Mayousse C, Celle C, Carella A and Simonato J P 2014 Synthesis and purification of long copper nanowires. Application to high performance flexible transparent electrodes with and without PEDOT:PSS *Nano Res.* **7** 315–24
[63] Kim Y-S, Chang M-H, Lee E-J, Ihm D-W and Kim J-Y 2014 Improved Electrical Conductivity of PEDOT-Based Electrode Films Hybridized with Silver Nanowires *Synth. Met.* **195** 69–74